Exact Extremal Statistics in the Classical 1D Coulomb Gas

Abhishek Dhar,[1] Anupam Kundu,[1] Satya N. Majumdar,[2] Sanjib Sabhapandit,[3] and Grégory Schehr[2]
[1]International Centre for Theoretical Sciences, TIFR, Bangalore 560089, India
[2]LPTMS, CNRS, Univ. Paris-Sud, Université Paris-Saclay, 91405 Orsay, France
[3]Raman Research Institute, Bangalore 560080, India
(Received 28 April 2017; published 8 August 2017)

We consider a one-dimensional classical Coulomb gas of N-like charges in a harmonic potential—also known as the one-dimensional one-component plasma. We compute, analytically, the probability distribution of the position $x_{\max}$ of the rightmost charge in the limit of large N. We show that the typical fluctuations of $x_{\max}$ around its mean are described by a nontrivial scaling function, with asymmetric tails. This distribution is different from the Tracy-Widom distribution of $x_{\max}$ for Dyson's log gas. We also compute the large deviation functions of $x_{\max}$ explicitly and show that the system exhibits a third-order phase transition, as in the log gas. Our theoretical predictions are verified numerically.

DOI: 10.1103/PhysRevLett.119.060601

The Tracy-Widom (TW) distribution has emerged ubiquitously in diverse systems in the recent past [1,2]. It was originally discovered as the limiting distribution of the top eigenvalue $x_{\max}$ of an $N \times N$ Gaussian random matrix [3]. Since then, it has appeared in various areas of physics [4,5], mathematics [6,7], and information theory [8]. For example, in physics it has appeared in stochastic growth models and related directed polymer in $1+1$ dimensional random media belonging to the Kardar-Parisi-Zhang (KPZ) universality class [9–15], nonintersecting Brownian motions [16], noninteracting fermions in a one-dimensional trapping potential [17–19], disordered mesoscopic systems [20] and even in the Yang-Mills gauge theory in two dimensions [16]. It has also been measured experimentally in several systems including liquid crystals [21], coupled fiber lasers [22], or disordered superconductors [23]. The TW distribution describes the probability of *typical* fluctuations of $x_{\max}$ around its mean. In contrast, the *atypical* fluctuations of $x_{\max}$ to the left and right, far from its mean, are described, respectively, by the left and right large deviation tails. These tails have been computed explicitly [24–28] and are shown to correspond to two different thermodynamic phases separated by a third-order phase transition [29,30]. Similar third-order phase transitions have also been found in a variety of other systems [30–36].

For Gaussian ensembles in random matrix theory (RMT), the joint probability distribution function (PDF) of the N real eigenvalues $\{x_1, \ldots, x_N\}$ is known explicitly [37,38]

$$\mathcal{P}(\{x_i\}) = B_N e^{-(\beta/2)(N\sum_{i=1}^{N} x_i^2 - \sum_{i\neq j}\log(|x_i - x_j|))}, \quad (1)$$

where B_N is a normalization constant and $\beta = 1$, 2, and 4 depending on the symmetries of the matrices [37,38]. This joint PDF can be interpreted as the equilibrium Gibbs distribution of a gas of N charges with positions x_i's that are confined on a line in the presence of an external harmonic potential and repelling each other via two-dimensional logarithmic Coulomb interactions. This system is known as Dyson's log gas [39]. In this picture the largest eigenvalue $x_{\max} = \max\{x_1, \ldots, x_N\}$ corresponds to the position of the rightmost particle. The average density of eigenvalues $\rho_N(x)$ converges for large N to the Wigner semicircular law, $\rho_\infty(x) \sim \sqrt{2 - x^2}/\pi$ which has a finite support $[-\sqrt{2}, +\sqrt{2}]$. Hence, the average $\langle x_{\max}\rangle \sim \sqrt{2}$ for large N. The typical fluctuations of $x_{\max}$ around its mean $\sqrt{2}$ are of $O(N^{-2/3})$. On this scale the cumulative distribution $Q(w, N) = \mathrm{Prob}(x_{\max} \leq w, N)$, takes the scaling form

$$Q(w, N) \approx \mathcal{F}_\beta(\sqrt{2}N^{2/3}(w - \sqrt{2})), \quad (2)$$

where $\mathcal{F}_\beta(x)$ is the Tracy-Widom distribution. This scaling function can be written in terms of the solution of a Painlevé II equation [3] and has non-Gaussian tails. Interestingly, even though the TW distribution was derived

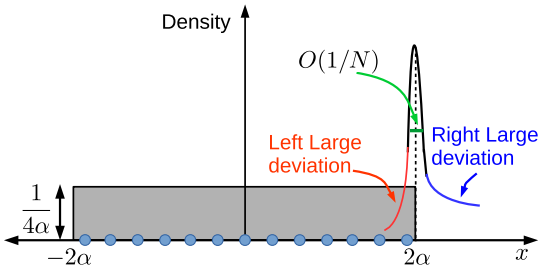

FIG. 1. Schematic plot of the PDF of $x_{\max}$ with a peak around the right edge 2α of the average density profile. The typical fluctuations (black) of $O(1/N)$ are described by $F'_\alpha(x)$ [see Eq. (7)], while the large deviations of $O(1)$ to the left and right of the mean are described by the left (red) and right (blue) large deviation tails.

originally for a harmonic confining potential, it has been shown to be universal with respect to the shape of the confining potential, as long as the average density vanishes at the upper edge as a square root (as in the case of the Wigner semicircular law). A natural question then arises whether the TW distribution for $x_{\max}$ is robust when one changes, instead of the confining potential, the nature of the repulsive interaction between the charges.

A natural candidate model to address this question is the system of one-dimensional charges in a harmonic potential but interacting pairwise via the true 1D Coulomb potential. The energy of this system is given by

$$E(\{x_i\}) = \frac{N^2}{2}\sum_{i=1}^{N} x_i^2 - \alpha N \sum_{i\neq j} |x_i - x_j|, \tag{3}$$

where $\alpha \geq 0$ denotes the strength of the Coulomb repulsion. The choice of the powers of N in the coupling constants is such that for large N (i) both terms in the energy are of same order and (ii) the charges are confined in a region whose span is $O(1)$. Indeed this is also the one-dimensional one-component plasma (1DOCP) or "jellium" model, where N charges of the same sign interact in the presence of a uniform background of opposite charges, assuring charge neutrality. This model is a paradigm for 1D charged plasma [40] as several observables can be calculated analytically [41–45].

In this Letter, we show that the statistics of the position of the rightmost charge $x_{\max}$ can also be computed exactly in this 1DOCP model. Our main result is to show that the limiting distribution of the typical fluctuations of $x_{\max}$ in this model is indeed different from the TW distribution, found in Dyson's log gas. Moreover, by computing the left and the right large deviation functions explicitly, we find that the third-order phase transition between a pushed gas (left large deviation) and a pulled gas (right large deviation) is still present in the 1DOCP model, as in the case of the log gas. Interestingly, a similar third-order phase transition between the pushed and the pulled phase was recently found [46] by analyzing large deviation functions associated with the position of the farthest charge in a d-dimensional jellium model, though the limiting distribution of the position of the farthest charge is still open for this d-dimensional problem. In $d = 1$ this corresponds to the distribution of the maximum of $|x_i|$'s of the charges.

We start with the joint PDF of the positions $x_i \in (-\infty, \infty)$ in the 1DOCP, given by the Boltzmann weight

$$\mathcal{P}(\{x_i\}) = \frac{1}{Z_N}\exp[-E(\{x_i\})], \tag{4}$$

where Z_N is the partition function and the energy $E(\{x_i\})$ is given in Eq. (3). In the large N limit, the average density can be obtained by minimizing the energy $E(\{x_i\})$. It is easy to show that the minimum energy configuration is given by $x_j^* = (2\alpha/N)(2j - N - 1)$ $(j = 1, \ldots, N)$. Hence, the particles are equispaced and the rightmost (leftmost) particle is at $x_N^* = 2\alpha(1 - 1/N)$ [respectively, at $x_1^* = -2\alpha(1 - 1/N)$]. This implies that in the $N \to \infty$ limit, the average density profile $\rho_\infty(x)$ is flat: $\rho_\infty(x) = (1/4\alpha)$ for $-2\alpha \leq x \leq 2\alpha$ (see Fig. 1), in contrast to the Wigner semicircle in the log gas. Our focus here is on the large N behavior of the cumulative distribution of the rightmost particle,

$$Q(w, N) = \text{Prob}[x_{\max} \leq w, N]. \tag{5}$$

To anticipate the scaling behavior of $Q(w, N)$, we first make the following observations. It follows from the above analysis of the average density that the mean position of the rightmost particle is at $\langle x_{\max}\rangle = x_N^* = 2\alpha(1 - 1/N)$. Given that the average density is uniform, the typical separation between two adjacent particles is of $O(1/N)$ everywhere. Hence, the scale of typical fluctuations of $x_{\max}$ around its average is also of $O(1/N)$. This suggests that the cumulative probability distribution $Q(w, N)$, in the region of typical fluctuations where $|w - 2\alpha| \sim O(1/N)$, should have the scaling form for large N, $Q(w, N) \approx F_\alpha[N(w - x_N^*)] = F_\alpha[N(w - 2\alpha) + 2\alpha]$ where $F_\alpha(x)$ is a nontrivial scaling function (the analogue of the TW distribution for the log gas). In this Letter, we compute this scaling function $F_\alpha(x)$. In addition, for atypical fluctuations where $x_{\max} - \langle x_{\max}\rangle \sim O(1)$, both to the left and to the right of the mean, $Q(w, N)$ has large deviation tails that are also computed explicitly. More precisely, we find

$$Q(w, N) \approx \begin{cases} e^{-N^3\Phi_-(w)+O(N^2)} & 0 < 2\alpha - w \sim O(1) \\ F_\alpha[N(w - 2\alpha) + 2\alpha] & |2\alpha - w| \sim O(1/N) \\ 1 - e^{-N^2\Phi_+(w)+O(N)} & 0 < w - 2\alpha \sim O(1), \end{cases} \tag{6}$$

where $\Phi_-(w)$ and $\Phi_+(w)$ are the left and right rate functions. We show that the scaling function $F_\alpha(x)$ in the central regime satisfies a nonlocal eigenvalue equation

$$\frac{dF_\alpha(x)}{dx} = A(\alpha)e^{-x^2/2}F_\alpha(x + 4\alpha), \tag{7}$$

with the boundary conditions $F_\alpha(-\infty) = 0$ and $F_\alpha(\infty) = 1$. These boundary conditions, along with the fact that $F_\alpha(x) \geq 0$ for all x, uniquely fix the eigenvalue $A(\alpha)$. Clearly, the scaling function $F_\alpha(x)$ is different from the TW distribution. While it is hard to compute $A(\alpha)$ explicitly for all $\alpha \geq 0$ [for a numerical plot of $A(\alpha)$, see Fig. 2], we can determine its small and large α behaviors: $A(\alpha) \to 1/(4e\alpha)$ as $\alpha \to 0$ and $A(\alpha) \to 1/\sqrt{2\pi}$ as $\alpha \to \infty$. From Eq. (7), we can derive the leading asymptotic tails of the PDF $F'_\alpha(x)$ for all α

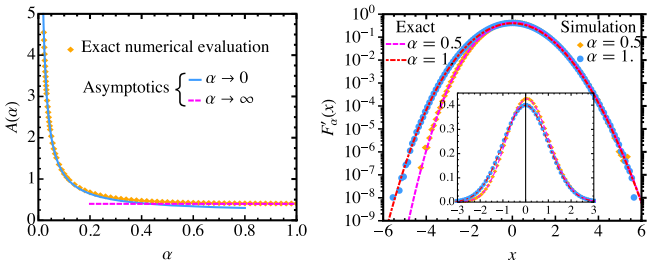

FIG. 2. (Left) Plot of $A(\alpha)$ and numerical verification of its $\alpha \to 0$ and $\alpha \to \infty$ asymptotic. (Right) Comparison of the theoretical $F'_\alpha(x)$ obtained by solving numerically Eq. (7) by a shooting method and $F'_\alpha(x)$ obtained from direct Monte Carlo simulation of the 1DOCP (with $N = 50$) for two different values of the coupling parameter, $\alpha = 1$ and $\alpha = 0.5$. Inset shows the distribution in the normal scale.

$$F'_\alpha(x) \approx \begin{cases} \exp[-|x|^3/24\alpha + O(x^2)] & \text{as } x \to -\infty \\ \exp[-x^2/2 + O(x)] & \text{as } x \to \infty. \end{cases} \quad (8)$$

We note that the leading $x \to -\infty$ behavior of $F'_\alpha(x)$ is identical to that of the TW distribution $\mathcal{F}'_{\beta=1/\alpha}(x)$, while the right tail of $F'_\alpha(x)$ decays faster than the TW right tail [47]. This is indeed our main result. In addition, we also compute exactly the large deviation rate functions. For the left tail we find

$$\Phi_-(w) = \begin{cases} \frac{(2\alpha - w)^3}{24\alpha}, & -2\alpha \le w \le 2\alpha \\ \frac{w^2}{2} + \frac{2}{3}\alpha^2, & w \le -2\alpha. \end{cases} \quad (9)$$

For the right tail, we find

$$\Phi_+(w) = \frac{(w - 2\alpha)^2}{2}, \qquad w > 2\alpha. \quad (10)$$

It is easy to check, using the asymptotic behavior of $F'_\alpha(x)$ for large $|x|$ in Eq. (8), that the central part of the distribution of $x_{\max}$ matches smoothly with the two large deviation regimes flanking this central part. Indeed, as discussed later, the vanishing of $\Phi_-(w)$ when $w \to 2\alpha$ as a cubic power is responsible for a third-order phase transition at the critical point $w = 2\alpha$, in very much the same way as in the log gas [30].

We start from the joint PDF of $\{x_i\}$'s in Eq. (4). We note that $Q(w, N) = \text{Prob}[x_{\max} \le w] = \text{Prob}(x_1 \le w, \ldots, x_N \le w)$. Hence it can be expressed as the ratio of two partition functions

$$Q(w, N) = \frac{Z_N(w)}{Z_N(\infty)}, \qquad \text{where ,} \quad (11)$$

$$Z_N(w) = \int_{-\infty}^{w} dx_1 \cdots \int_{-\infty}^{w} dx_N e^{-E(\{x_i\})}, \quad (12)$$

with $E(\{x_i\})$ given in Eq. (3) and we have suppressed the α dependence in $Z_N(w)$ for simplicity. Note that $Z_N(w)$ can be interpreted as the partition function of the 1DOCP in the presence of a hard wall at w. Below, we analyze $Q(w, N)$ in the central regime first, followed by the two large deviation tails.

Central regime.—Noting that the energy function $E(\{x_i\})$ in Eq. (3) is symmetric under permutations over the positions $(x_1, x_2, \ldots, x_N)$, we write

$$Z_N(w) = N! \prod_{k=1}^{N} \int_{-\infty}^{w} dx_k \; e^{-E(\{x_k\})} \prod_{j=2}^{N} \Theta(x_j - x_{j-1}), \quad (13)$$

where $\Theta(x)$ is the Heaviside theta function. For an ordered configuration $(x_1 < x_2 < \cdots < x_N)$, one can eliminate the absolute values $|x_i - x_j|$ and rewrite the energy function $E(\{x_i\})$ in Eq. (3) as $E(\{x_i\}) = (N^2/2)\sum_{i=1}^{N}[x_i - (2\alpha/N)(2i - N - 1)]^2 + C_N(\alpha)$, where $C_N(\alpha) = 2\alpha^2 \sum_{i=1}^{N}(2i - N - 1)^2$ is just a constant. This trick of eliminating the absolute values via ordering has been used before for 1DOCP in numerous contexts [41,43–45]. Performing a change of variables $\xi_k = [Nx_k - 2\alpha(2k - N - 1)]$ for all $k = 1, 2, \ldots, N$ in Eq. (13), we can rewrite $Z_N(w) = N! D_\alpha(N[w - (2\alpha/N)(N - 1)], N)$ where

$$D_\alpha(x, N) = \int_{-\infty}^{x} d\xi_N \int_{-\infty}^{\xi_N + 4\alpha} d\xi_{N-1} \cdots \int_{-\infty}^{\xi_2 + 4\alpha} d\xi_1 \times e^{-\frac{1}{2}\sum_{i=1}^{N}\xi_i^2}. \quad (14)$$

Therefore setting $x = N[w - (2\alpha/N)(N - 1)]$, $Q(w, N)$ in Eq. (11) can be written as

$$Q(w, N) = \frac{D_\alpha(x, N)}{D_\alpha(\infty, N)} \equiv F_\alpha(x, N). \quad (15)$$

Taking the derivative with respect to x in Eq. (15), and using Eq. (14), we obtain

$$\frac{dF_\alpha(x, N)}{dx} = \frac{D_\alpha(\infty, N - 1)}{D_\alpha(\infty, N)} e^{-(x^2/2)} F_\alpha(x + 4\alpha, N - 1). \quad (16)$$

To estimate the ratio $D_\alpha(\infty, N - 1)/D_\alpha(\infty, N)$ for large N, we note from Eq. (14) that $D_\alpha(\infty, N)$ can be interpreted as the partition function of an auxiliary gas of particles with positions $\xi_1, \xi_2, \ldots, \xi_N$ confined in an external harmonic potential and with the one-sided constraint $\xi_{k-1} < \xi_k + 4\alpha$ for all $k = 2, 3, \ldots, N$. Indeed this constraint provides a short-range interaction between the particles. Thus our original problem of the 1DOCP which has long-range interaction is mapped onto a problem of short-ranged interacting particles. For such a short-ranged system, it is natural to expect that the free energy is extensive in N. Thus one would expect that, for large N, the partition function must scale as $D_\alpha(\infty, N) \sim [A(\alpha)]^{-N}$ where $\ln A(\alpha)$ is the free energy per particle. Thus

the ratio $D_\alpha(\infty, N-1)/D_\alpha(\infty, N) \to A(\alpha)$ as $N \to \infty$. This suggests that $F_\alpha(x, N)$ should converge to a limiting form $F_\alpha(x)$ for large N, which then satisfies the nonlocal eigenvalue Eq. (7). Thus the eigenvalue $A(\alpha)$ has a physical interpretation: $\ln A(\alpha)$ is the free energy per particle of a short-ranged interacting gas. However, computing analytically $A(\alpha)$ for all α seems hard. Interestingly, Baxter [43] encountered a similar nonlocal eigenvalue equation while computing the partition function of the 1DOCP in a finite box $[-L, +L]$ and analyzed the eigenvalue $A(\alpha)$ in the two limits $\alpha \to 0$ and $\alpha \to \infty$. Translating his results to our problem, following a simple rescaling of the parameters, we obtain the asymptotic results for $A(\alpha)$ announced before.

It is straightforward to derive the asymptotic tails of $F'_\alpha(x)$ in Eq. (8). We consider first the limit $x \to \infty$ where $F_\alpha(x+4\alpha) \to 1$ on the right-hand side (rhs) of Eq. (8). Hence, to leading order, $F'_\alpha(x) \approx A(\alpha) e^{-x^2/2}$, providing the Gaussian right tail in Eq. (8). To compute the left tail, we make a simple ansatz that $F_\alpha(x) \approx e^{-a_0|x|^\delta}$ as $x \to -\infty$, where a_0 and δ are to be determined. Substituting this ansatz in the rhs of Eq. (7) yields $\approx A(\alpha) e^{-x^2/2 - a_0(|x|-4\alpha)^\delta}$. For large $|x|$, $(|x|-4\alpha)^\delta \sim |x|^\delta (1 - 4\alpha\delta/|x|)$ to leading orders. Hence the rhs behaves as $A(\alpha) e^{-a_0|x|^\delta - x^2/2 + 4\alpha\delta|x|^{\delta-1}}$. The left-hand side (lhs) of Eq. (7) behaves as $\approx e^{-a_0|x|^\delta}$ to leading order. Comparing both sides, we see that the term $x^2/2$ and $|x|^{\delta-1}$ on the rhs must cancel each other implying $\delta = 3$ and $a_0 = 1/(8\alpha\delta) = 1/(24\alpha)$. This provides the leading left tail of $F'_\alpha(x)$ in Eq. (8).

For general $\alpha > 0$, determining explicitly the eigenvalue $A(\alpha)$ and the full scaling function $F_\alpha(x)$ is difficult. However, they can be obtained by solving Eq. (7) numerically by tuning the value of $A(\alpha)$ using the standard shooting method. This gives $F_\alpha(x)$ and $A(\alpha)$ simultaneously. In Fig. 2 (left panel), we plot $A(\alpha)$ vs α and compare with its predicted asymptotics. In Fig. 2 (right panel), we compare $F'_\alpha(x)$ evaluated numerically from this shooting method, with the one obtained from direct Monte Carlo simulation of the 1DOCP. The agreement is excellent.

Left large deviation function.—We consider $Q(w, N)$ in Eqs. (11) and (12) with $0 < 2\alpha - w \sim O(1)$. Since w represents the position of the hard wall, $w < 2\alpha$ corresponds to "pushing" the charges to the left of the right edge at 2α. This disturbs the originally flat density and leads to a collective reorganization of all the charges, as in the case of the log gas [25,26]. We get instead a new equilibrium density that minimizes the energy, i.e., a new saddle point of the integral in Eq. (12). It is well known that in the jellium model, the bulk density is insensitive to the location of a wall [48]. This implies that in the bulk, the density is still given by the original equilibrium value $1/(4\alpha)$, for $-2\alpha < w \le 2\alpha$. Hence, when the wall moves to the left of 2α, all the charges that get pushed by the wall must get absorbed *at* the wall. This observation leads us to look for a saddle point density of the form

$$\rho_w(x) = \frac{1}{4\alpha} + C\delta(x-w), \qquad -B \le x \le w, \quad (17)$$

where the constant bulk density is supported over the interval $[-B, w]$. We then minimize the energy with respect to the two variational parameters B and C. Skipping details (see Ref. [49]), we find that

$$C = 1/2 - w/(4\alpha), \qquad B = 2\alpha, \quad (18)$$

as long as $-2\alpha \le w \le 2\alpha$. When w hits -2α from the right, all the charges get absorbed at the wall w and the saddle point density is just $\rho_w(x) = \delta(x-w)$, for all $w \le -2\alpha$. Substituting $\rho_w(x)$ in the energy [49], we find the results for $\Phi_-(w)$ given in Eq. (9).

Right large deviations.—For fluctuations $(x_{\max} - 2\alpha) \sim O(1)$ to the right of the edge 2α, we consider the PDF $\partial_w Q(w, N)$ in Eqs. (11) and (12) with $w > 2\alpha$. It turns out that the configuration that dominates this integral is one where the rightmost charge is at $w > 2\alpha$, while the rest of the $N-1$ charges stay in the equilibrium configuration with a flat profile over the interval $[-2\alpha, +2\alpha]$. This is analogous to the "pulled" phase in the log gas [27]. Thus, for large N, the PDF can be approximated as $\partial_w Q(w, N) \approx e^{-\Delta E_{\rm pulled}}$, where $\Delta E_{\rm pulled}$ is the energy cost of pulling the rightmost particle from the "sea" of $N-1$ particles in the equilibrium flat configuration. This energy cost can be estimated from Eq. (3): a first contribution from the change in the external potential energy of the rightmost charge and a second due to the interaction of the rightmost charge with the $(N-1)$ other particles. One gets (see Ref. [49] for details) $\Delta E_{\rm pulled} \approx N^2[(w^2/2) - \frac{1}{2}\int_{-2\alpha}^{2\alpha}(w-x)dx]$ up to a constant. This gives $\partial_w Q_N(w) \approx e^{-N^2\Phi_+(w)}$ where $\Phi_+(w)$ is given in Eq. (10).

Since $Q(w, N)$ is the ratio of two partition functions [Eq. (11)], $-\ln Q(w, N)$ is the free energy difference between the pushed (left) and the pulled (right) phase. From Eq. (6), this free energy $\propto \Phi_-(w)$ has a singular behavior at the critical point $w = 2\alpha$. Indeed it vanishes as a cubic power as $w \to 2\alpha$ from the left [see Eq. (9)], leading to a discontinuity of the third derivative of $\Phi_-(w)$ at $w = 2\alpha$. This third-order phase transition at $w = 2\alpha$ is similar to the one in the log gas. Unlike in the log gas, there is an additional third-order phase transition in this 1DOCP when $w \to -2\alpha$ [see Eq. (9)]. However, this transition is not of the "pushed-pulled" type like the one at $w = 2\alpha$, but rather a condensation-type transition as all charges accumulate at the wall for $w \le -2\alpha$.

Conclusion.—In this Letter we have studied analytically the distribution of the position of the rightmost particle $x_{\max}$ of a 1D Coulomb gas confined in an external harmonic potential (1DOCP), in the limit of a large number of particles N. We have obtained the limiting large N distribution describing the typical fluctuations of $x_{\max}$ around its mean, and shown that it is different from the Tracy-Widom distribution of the log gas. We also computed

the rate functions associated with atypically large fluctuations around the mean and found a third-order phase transition between a pushed and a pulled phase, as in the log gas. Our work raises several interesting questions. For instance, how universal is the limiting distribution of $x_{\max}$ if one changes the confining potential or the pairwise repulsive interaction? It would be challenging to study $x_{\max}$ with a repulsive interaction of the form $|x_i - x_j|^{-k}$ (where $k \to 0$ corresponds to log gas, while $k = -1$ corresponds to the 1DOCP). Unlike the log gas, the 1DOCP does not have a determinantal structure and computing its n-point correlations would be interesting.

We thank M. Krishnapur, D. Mukamel, E. Trizac, and P. Vivo for discussions. We acknowledge support from the Indo-French Centre for the Promotion of Advanced Research (IFCPAR) under Project No. 5604-2.

[1] M. Buchanan, Nat. Phys. **10**, 543 (2014).
[2] N. Wolchover, Quanta Mag. (2014), https://lc.cx/Z9ao.
[3] C. A. Tracy and H. Widom, Commun. Math. Phys. **159**, 151 (1994); C. A. Tracy and H. Widom, Commun. Math. Phys. **177**, 727 (1996).
[4] S. N. Majumdar, *Les Houches Lecture Notes on Complex Systems*, edited by J.-P. Bouchaud, M. Mézard, and J. Dalibard (Elsevier, Amsterdam, 2007).
[5] T. Kriecherbauer and J. Krug, J. Phys. A **43**, 403001 (2010).
[6] J. Baik, P. Deift, and K. Johansson, J. Am. Math. Soc. **12**, 1119 (1999).
[7] I. M. Johnstone, Ann. Stat. **29**, 295 (2001).
[8] P. Kazakopoulos, P. Mertikopoulos, A. L. Moustakas, and G. Caire, IEEE Trans. Inf. Theory **57**, 1984 (2011).
[9] K. Johansson, Commun. Math. Phys. **209**, 437 (2000).
[10] M. Prähofer and H. Spohn, Phys. Rev. Lett. **84**, 4882 (2000).
[11] S. N. Majumdar and S. Nechaev, Phys. Rev. E **69**, 011103 (2004).
[12] T. Sasamoto and H. Spohn, Phys. Rev. Lett. **104**, 230602 (2010).
[13] P. Calabrese, P. Le Doussal, and A. Rosso, Europhys. Lett. **90**, 20002 (2010).
[14] V. Dotsenko, Europhys. Lett. **90**, 20003 (2010).
[15] G. Amir, I. Corwin, and J. Quastel, Commun. Pure Appl. Math. **64**, 466 (2011).
[16] P. J. Forrester, S. N. Majumdar, and G. Schehr, Nucl. Phys. **B844**, 500 (2011).
[17] V. Eisler, Phys. Rev. Lett. **111**, 080402 (2013).
[18] D. S. Dean, P. Le Doussal, S. N. Majumdar, and G. Schehr, Phys. Rev. Lett. **114**, 110402 (2015).
[19] D. S. Dean, P. Le Doussal, S. N. Majumdar, and G. Schehr, Phys. Rev. A **94**, 063622 (2016).
[20] M. G. Vavilov, P. W. Brouwer, V. Ambegaokar, and C. W. J. Beenakker, Phys. Rev. Lett. **86**, 874 (2001).
[21] K. A. Takeuchi, M. Sano, T. Sasamoto, and H. Spohn, Sci. Rep. **1**, 34 (2011).
[22] M. Fridman, R. Pugatch, M. Nixon, A. A. Friesem, and N. Davidson, Phys. Rev. E **85**, R020101 (2012).
[23] G. Lemarié, A. Kamlapure, D. Bucheli, L. Benfatto, J. Lorenzana, G. Seibold, S. C. Ganguli, P. Raychaudhuri, and C. Castellani, Phys. Rev. B **87**, 184509 (2013).
[24] G. Ben Arous, A. Dembo, and A. Guionnet, Probab. Theory Relat. Fields **120**, 1 (2001).
[25] D. S. Dean and S. N. Majumdar, Phys. Rev. Lett. **97**, 160201 (2006).
[26] D. S. Dean and S. N. Majumdar, Phys. Rev. E **77**, 041108 (2008).
[27] S. N. Majumdar and M. Vergassola, Phys. Rev. Lett. **102**, 060601 (2009).
[28] G. Borot, B. Eynard, S. N. Majumdar, and C. Nadal, J. Stat. Mech. (2011) P11024.
[29] C. Nadal and S. N. Majumdar, J. Stat. Mech. (2011) P04001.
[30] S. N. Majumdar and G. Schehr, J. Stat. Mech. (2014) P01012.
[31] G. Schehr, S. N. Majumdar, A. Comtet, and P. J. Forrester, J. Stat. Phys. **150**, 491 (2013).
[32] F. Colomo and A. G. Pronko, Phys. Rev. E **88**, 042125 (2013).
[33] R. Allez, J. Touboul, and G. Wainrib, J. Phys. A **47**, 042001 (2014).
[34] F. D. Cunden, F. Mezzadri, and P. Vivo, J. Stat. Phys. **164**, 1062 (2016).
[35] P. Le Doussal, S. N. Majumdar, and G. Schehr, Europhys. Lett. **113**, 60004 (2016).
[36] P. Sasorov, B. Meerson, and S. Prolhac, J. Stat. Mech. (2017) 063203.
[37] M. L. Mehta, *Random Matrices*, 2nd ed. (Academic Press, New York, 1991).
[38] P. J. Forrester, *Log-Gases and Random Matrices* (Princeton University Press, Princeton, NJ, 2010).
[39] F. J. Dyson, J. Math. Phys. **3**, 140; **3**, 157 (1962); **3**, 166 (1962).
[40] P. Choquard, H. Kunz, P. A. Martin, and M. Navet, in *Physics in One Dimension* (Springer, Berlin, Heidelberg, 1981), pp. 335–350.
[41] A. Lenard, J. Math. Phys. (N.Y.) **2**, 682 (1961).
[42] S. Prager, in *The One-Dimensional Plasma, in Advances in Chemical Physics*, edited by I. Prigogine (John Wiley & Sons, Inc., Hoboken, NJ, USA, 1962), Vol. 4, p. 201.
[43] R. J. Baxter, Proc. Cambridge Philos. Soc. **59**, 779 (1963).
[44] D. S. Dean, R. R. Horgan, A. Naji, and R. Podgornik, Phys. Rev. E **81**, 051117 (2010).
[45] G. Téllez and E. Trizac, Phys. Rev. E **92**, 042134 (2015).
[46] F. D. Cunden, P. Facchi, M. Ligabò, and P. Vivo, J. Stat. Mech. (2017) 053303.
[47] L. Dumaz and B. Virág, Ann. Inst. Henri Poincaré Probab. Statist. **49**, 915 (2013).
[48] S. N. Armstrong, S. Serfaty, and O. Zeitouni, Potential analysis **41**, 945 (2014).
[49] See Supplemental Material at http://link.aps.org/supplemental/10.1103/PhysRevLett.119.060601 for more details.